Phase Separation Behavior of Poly(methyl methacrylate-*co*-dimethylaminoethyl methacrylate)/Methyl Silsesquioxane Hybrid Nanocomposites Studied by Dansyl Fluorescence

Q. R. Huang,*[,†,‡] Curtis W. Frank,*[,†] David Mecerreyes,[§] Willi Volksen,[§] and Robert D. Miller*[,§]

Department of Chemical Engineering, Stanford University, Stanford, California 94305, Department of Food Science, Rutgers University, New Brunswick, New Jersey 08901, and IBM Almaden Research Center, 650 Harry Road, San Jose, California 95120

Received July 27, 2004. Revised Manuscript Received November 24, 2004

Ultralow dielectric constant (k) materials ($k < 2.0$) are generally prepared by the sacrificial macromolecular porogen route. Dansyl steady-state and time-resolved fluorescence have been used to study the phase separation behavior of methyl silsesquioxane (MSSQ) and poly(methyl methacrylate-*co*-dimethylaminoethyl methacrylate) [P(MMA-*co*-DMAEMA)] hybrid nanocomposites, which are promising candidates for spin-on, ultralow dielectric constant applications. Resins MSSQ-HI and MSSQ-LO, which differ mainly in the concentration of −SiOH (silanol) present in the uncured samples, are used to study the effect of endgroup functionality on the phase separation behavior of the hybrid nanocomposites. Fluorescence results reveal that, for MSSQ-LO resin, a single emission band located in the range of 428−456 nm is observed for P(MMA-*co*-DMAEMA) loading levels up to 20 wt %. With further increase in polymer loading, a second emission band located at higher emission energy ranging from 408 to 422 nm appears, and the amount of this higher energy band increases with polymer loading. By contrast, for MSSQ-HI, the composition-dependent high-energy band does not appear until polymer loading levels exceed 50 wt %. We infer information about local environment from the emission band position with the low-energy band associated with dansyl surrounded by MSSQ, and the composition-dependent high-energy band associated with dansyl surrounded by P(MMA-*co*-DMAEMA). Thus, our fluorescence results suggest that both increasing the polymer loading level and lowering the amount of silanol endgroup in the uncured MSSQ promote phase separation in the hybrid nanocomposites. This is evidenced by the increase in the proportion of the high-energy band, which we interpret as indicating that the probe molecules avoid the phase boundary region and seek a polymer-rich environment. This migration results in the formation of larger polymer domains and ultimately translates into larger size pores upon polymer burnout. Our interpretation is consistent with previous pyrene fluorescence, small angle neutron scattering, transmission electron microscopy, and small-angle X-ray scattering results.

Introduction

The miniaturization of microelectronic devices to sub-100-nm dimensions generally results in substantial increase in interconnect delays (RC delay) caused by increased line resistance (R) and capacitive (C) coupling, and crosstalk between the smaller and more closely spaced metal lines. Two approaches exist to mitigate an increase in RC delays: switching from aluminum to copper for interconnect metallurgy to reduce the wiring resistance, and replacing the traditional SiO_2 ($k \approx 4.0$) insulator with a significantly lower dielectric constant material to reduce the capacitance. Current production features have already reached 130 nm and are projected to decrease to 100 nm by the year 2006, according to the National Technology Road Map.[1] If we assume a dielectric scaling that is commensurate with the generational decrease in wiring dimension and pitch, dielectric constant targets of 2.6−2.9 and 2.0−2.2 for the 130 and 100 nm technology nodes, respectively, are required.

The search for ultralow k ($k < 2.2$) materials has attracted much interest in recent years.[2] For nonfluorinated materials, dielectric constants below 2.2 are almost inaccessible without introducing porosity. Porous materials are of interest to both industrial and academic groups because of their applications in areas such as ultralow dielectric constant films in the microelectronics industry,[2] the preparation of high-surface-area substrates for chemical/bio sensors,[3] and usage as

* To whom all correspondence should be addressed. E-mail: qhuang@aesop.rutgers.edu.
† Stanford University.
‡ Rutgers University.
§ IBM Almaden Research Center.

(1) *The National Technology Road map for Semiconductors*; Semiconductor Industry Association: San Jose, CA, 1997.
(2) (a) Miller, R. D. *Science* **1999**, *286*, 421. (b) Maier, G. *Prog. Polym. Sci.* **2001**, *26*, 3. (c) Hedrick, J. L.; Carter, K. R.; Labadie, J. W.; Miller, R. D.; Volksen, W.; Hawker, C. J.; Yoon, D. Y.; Russell, T. P.; McGrath, J. E.; Briber, R. M. *Adv. Polym. Sci.* **1999**, *141*, 1. (d) *Low-Dielectric Constant Materials*; Materials Research Society Symposia Proceedings, Pittsburgh, PA; Materials Research Society, 1995; Vol. 381; 2nd, 1996; Vol. 443; 3rd, 1997; Vol. 476; 4th, 1998; Vol. 511; 5th, 1999; Vol. 565. (e) Hawker, C. J.; Hedrick, J. L.; Miller, R. D.; Volksen, W.; *MRS Bull.* **2000**, *25*, 54.

10.1021/cm048774s CCC: $30.25
Published on Web 02/17/2005

catalysts,[4] gas-separation membranes,[5] and in photonic materials.[6] Nanoporous insulators can be created through sol−gel polymerization, based on the hydrolysis and condensation of organosilicate precursors such as metal halides and alkoxides, to form an interconnected three-dimensional network.[7]

To be used as ultralow *k* materials, the average pore diameter inside the porous insulators should be 15 nm or less. However, controlling the pore size and shape through sol−gel reactions to achieve the desired morphology presents a considerable challenge. Three methods have been commonly used to produce porous silica: (1) surfactant-templated hydrolysis/condensation of orthosilicate esters such as TEOS and TMOS with the use of cationic, nonionic, and polymeric surfactants, followed by the thermal removal of the surfactants;[8] (2) formation of optically clear nanocomposites of organosilicates with compatible organic polymers through specific interactions such as hydrogen bonding and/or ionic interactions;[9] and (3) use of spherical nanoparticles of polystyrene containing various surface functionalities along with templated hydrolysis/condensation of TEOS resulting in porous silica containing spherical pores equivalent to the size of the original polystyrene nanoparticles.[10] No matter which method is used, the final pore morphology in porous insulators is essentially determined by the polymer domain sizes that are controlled by the phase separation processes before the polymer burnout. It is necessary to have techniques that are sensitive to the nanosize scales in order to understand the phase separation behavior occurring in the organic−inorganic hybrid nanocomposites. In this paper, we show that fluorescence spectroscopy becomes the method of choice due to its convenience and intrinsic sensitivity.[11] Compared with solid-state NMR,[12] small-angle neutron scattering,[13] small-angle X-ray scattering,[14] differential scanning calorimetry,[15] dynamic mechanical analysis,[16] and dielectric spectroscopy,[17] the advantages of fluorescence spectroscopy lie in its low cost as well as its high sensitivity to local microenvironments.

One promising organosilicate resin for the ultralow-*k* applications is methyl silsesquioxane (MSSQ) with the general formula $(MeSiO_{3/2})_n$. Fully cured MSSQ is intrinsically hydrophobic, thermally stable at temperatures higher than 450 °C, and has dielectric constant substantially lower than that of silica (2.6−2.9 vs 4.0). For these reasons, MSSQ has attracted considerable attention in recent years as an alternative to silicon dioxide, and substantial effort has been made to develop routes for generating nanoporous MSSQ.[9,18]

Previously, star-shaped[18a] and hyperbranched[18b] poly(ϵ-caprolactone) (PCL), poly(alkylene ether) homo or copolymers, and nanoparticles produced by intramolecular crosslinking of linear polystyrene, methyl methacrylate, and caprolactone containing pendant polymerizable acrylate functionality by free radical initiation in ultradilute solutions,[18f] have been used to produce nanoporous MSSQ. Examples of poly(alkylene ether) materials include poly(propylene glycol) (PPG), poly(ethylene oxide) (PEO), PPG-*co*-PEO,[18c,d] and PEO-*block*-PPO-*block*-PEO.[18e] Very recently, linear random copolymers of poly(methyl methacrylate-*co*-dimethylaminoethyl methacrylate [P(MMA-*co*-DMAEMA)], produced by the radical copolymerization of methyl methacrylate (MMA) and *N*,*N*-dimethylaminoethyl methacrylate (DMAEMA), have successfully been used to generate nanoporous MSSQ.[9] Our interest in P(MMA-*co*-DMAEMA) originates from the fact that the porous MSSQ films formed

(3) (a) Rottman, C.; Grader, G.; DeHazan, Y.; Melchior, S.; Avnir, D. *J. Am. Chem. Soc.* **1999**, *121*, 8533. (b) Dantas de Morais, T.; Chaput, F.; Bailot, J.-P.; Lahlil, K.; Darracq, B.; Levy, Y. *Adv. Mater.* **1999**, *11*, 107. (c) Fidanza, J. Glazer, M.; Mutnick, D.; McGall, G.; Frank, C. W. *Nucleosides, Nucleotides Nucleic Acids* **2001**, *20*, 533.

(4) (a) Lev, O.; Tsionsky, M.; Rabinovich, L.; Glezer, V.; Sampath, S.; Pankratov, I.; Gun, J. *Anal. Chem.* **1995**, *67*, 22A. (b) Harmer, M. A.; Farneth, W. E.; Sun, Q. *J. Am. Chem. Soc.* **1996**, *118*, 7708. (c) Schubert, U. *New J. Chem.* **1994**, *18*, 1049.

(5) (a) Guizard, C.; Lacan, P. *New J. Chem.* **1994**, *18*, 1097. (b) Smaihi, M.; Jermoumi, T.; Marignan, J.; Noble, R. D. *J. Membr. Sci.* **1996**, *116*, 211.

(6) (a) Beecroft, L. L.; Ober, C. K. *Chem. Mater.* **1997**, *9*, 1302. (b) Klein, L. C. *Sol−Gel Optics, Processing and Applications*; Kluwer: Boston, 1994. (c) Sanchez, C.; Lebeau, B. *MRS Bull.* **2001**, *26*, 377.

(7) Brinker, C. J.; Scherer, G. W. *Sol−Gel Science: The Physics and Chemistry of Sol−Gel Processing*; Academic Press: San Diego, CA, 1990.

(8) (a) Zhao, D. Y.; Huo, Q. S.; Feng, J. L.; Chmelka, B. F.; Stucky, G. D. *J. Am. Chem. Soc.* **1998**, *120*, 6025. (b) Zhao, D. Y.; Huo, Q. S.; Feng, J. L.; Milosh, N.; Fredrickson, G. H.; Chmelka, B. F.; Stucky, G. D. *Science* **1998**, *279*, 548. (c) Yang, P. D.; Zhao, D. Y.; Chmelka, B. F.; Stucky, G. D. *Chem. Mater.* **1998**, *10*, 2033. (d) Yun, H.; Miyazawa, K.; Zhao, H.; Honma, I.; Kuwabara, M. *Adv. Mater.* **2001**, *13*, 1377.

(9) (a) Huang, Q. R.; Frank, C. W.; Mecerreyes, D.; Miller, R. D. *Polym. Mater. Sci. Eng.* **2001**, *84*, 792. (b) Huang, Q. R.; Volksen, W.; Huang, E.; Toney, M.; Frank, C. W.; Miller, R. D. *Chem. Mater.* **2002**, *14*, 3676.

(10) Antonietti, M.; Berton, B.; Göltner, C.; Hentz, H.-P. *Adv. Mater.* **1998**, *10*, 154.

(11) (a) Birks, J. B. *Photophysics of Aromatic Molecules*; Wiley-Interscience: New York, 1970. (b) Lakowicz, J. R. *Principles of Fluorescence Spectroscopy*, 2nd ed.; Plenum Press: New York, 1999.

(12) (a) Lin, T. S.; Ward, T. C. *Polym. Prepr.* **1983**, *24* (2), 136. (b) Clauss, J.; Schmidtrohr, K.; Spiess, H. W. *Acta Polym.* **1993**, *44*, 1. (c) VanderHart, D. L.; McFadden, G. B. *Solid State Nucl. Magn. Reson.* **1996**, *7*, 45. (d) Bauer, F.; Ernst, H.; Decker, U.; Findeisen, M.; Flasel, H.-J.; Langguth, H.; Hartmann, E.; Mehnert, R.; Peuker, C. *Macromol. Chem. Phys.* **2000**, *201*, 2654.

(13) (a) Yang, G. Y.; Briber, R. M.; Huang, E.; Rice, P. M.; Volksen, W.; Miller, R. D. *Polym. Mater. Sci. Eng.* **2001**, *85*, 18. (b) Higgins, J. S.; Benoit, H. C. *Polymers and Neutron Scattering*, Oxford University Press: Oxford, England, 1996.

(14) (a) Dahmouche, K.; Santilli, C. V.; Pulcinelli, S. H.; Craievich, A. F. *J. Phys. Chem. B.* **1999**, *103*, 4937. (b) Rodrigues, D. E.; Brennan, A. B.; Betrabet, C.; Wang, B.; Wilkes, G. L. *Chem. Mater.* **1992**, *4*, 1437. (3) Hedstrom, J. A.; Toney, M. F.; Huang, E.; Kim, H. C.; Volksen, W.; Magbitang, T.; Miller, R. D. *Langmuir* **2004**, *20*, 1535.

(15) (a) Chen, T. K.; Tien, Y. L.; Wei, K. H. *Polymer* **2000**, *41*, 1345. (b) Lee, Andre; Lichtenhan, J. D. *J. Appl. Polym. Sci.* **1999**, *73*, 1993.

(16) (a) Young, S. K.; Mauritz, K. A. *J. Polym. Sci., Part B: Polym. Phys.* **2001**, *39*, 1282. (b) Shelley, J. S.; Mather, P. T.; DeVries, K. L. *Polymer* **2001**, *42*, 5849. (c) Suh, D. J.; Lim, Y. T.; Park, O. O. *Polymer* **2000**, *41*, 8557.

(17) (a) Anastasiadis, S. H.; Karatasos, K.; Vlachos, G.; Manias, E.; Giannelis, E. P. *Mater. Res. Soc. Symp. Proc.* **1999**, *543*, 125. (b) Anastasiadis, S. H.; Karatasos, K.; Vlachos, G.; Manias, E.; Giannelis, E. P. *Phys. Rev. Lett.* **2000**, *84*, 915.

(18) (a) Nguyen, C. N.; Carter, K. R.; Hawker, C. J.; Hedrick, J. L.; Jaffe, R. L.; Miller, R. D.; Remenar, J. F.; Rhee, H.-W.; Rice, P. M.; Toney, M. F.; Trollsås, M.; Yoon, D. Y. *Chem. Mater.* **1999**, *11*, 3080. (b) Nguyen, C. N.; Hawker, C. J.; Miller, R. D.; Huang, E.; Hedrick, J. L.; Gauderon, R.; Hilborn, J. G. *Macromolecules* **2000**, *33*, 4281. (c) Carter, K. R.; Dawson, D. J.; DiPietro, R. A.; Hawker, C. J.; Hedrick, J. L.; Miller, R. D.; Yoon, D. Y. US Patent 5,895,263, 1999. (d) Hawker, C. J.; Hedrick, J. L.; Miller, R. D.; Volksen, W. U.S. Patent 6,107,357, 2000. (e) Yang, S.; Mirau, P. A.; Pai, C.-S.; Nalamasu, O.; Reichmanis, E.; Pai, J. C.; Obeng, Y. S.; Seputro, J.; Lin, E. K.; Lee, H. J.; Gidley, D. W.; Sun, J. N. *Chem. Mater.* **2001**, *13*, 2762. (f) Mecerreyes, D.; Lee, V.; Hawker, C. J.; Hedrick, J. L.; Wursch, A.; Volksen, W.; Magbitang, T.; Huang, E.; Miller, R. D. *Adv. Mater.* **2001**, *13*, 204.

by using P(MMA-*co*-DMAEMA) as a porogen show superior film-coating quality, and such defect-free films are required for on-chip insulator applications. Copolymers containing at least 15 mol % DMAEMA are highly miscible in uncured MSSQ films, and high-quality, defect-free, ultralow-k ($k <$ 2.0) nanoporous MSSQ thin films are produced upon polymer burnout. On the basis of our experience, P(MMA-*co*-DMAEMA) containing 20−30 mol % of DMAEMA comonomer provides optimal coatings and foaming efficiencies.[9]

Our previous study on MSSQ/P(MMA-*co*-DMAEMA) hybrid nanocomposites showed that the miscibility between MSSQ and P(MMA-*co*-DMAEMA) was due to the strong hydrogen bonding interactions between −SiOH end groups in MSSQ before MSSQ cross-linking and the tertiary amino substituent in P(MMA-*co*-DMAEMA).[9] The average pore sizes in porous MSSQ are partly determined by the initial MSSQ end group functionality: i.e., at similar porogen loading levels, resins with relatively more SiOH (silanol) functionality initially yield substantially smaller pore sizes. To develop a molecular-level understanding of the phase separation occurring in MSSQ/P(MMA-*co*-DMAEMA) hybrid nanocomposites, we carried out modulated differential scanning calorimetry (MDSC) and pyrene fluorescence studies of the miscibility in MSSQ and P(MMA-*co*-DMAEMA) hybrid nanocomposites.[19] MDSC results showed the existence of a single glass transition temperature (T_g) for P(MMA-*co*-DMAEMA) loading levels up to 70 wt %, indicating apparent miscibility for length scales of 10 nm and above. The existence of a single T_g may also be due to the fact that MDSC is not sensitive enough to distinguish two phase separated domains with similar T_g. Complementary results were obtained from pyrene excimer fluorescence, which occurs when an electronically excited-state pyrene approaches within about 4 Å of a ground-state pyrene in the proper geometry. The excimer-to-monomer (I_E/I_M) ratios for the MSSQ with higher initial silanol concentration were higher compared to those of the MSSQ with low silanol concentration at the same polymer loading, suggesting the formation of larger polymer domains for the former. However, the application of pyrene excimer fluorescence is limited by the fact that it is insensitive to hybrid nanocomposites with polymer domain sizes larger than ∼5 nm.[19]

In an effort to further the exploration of photophysical approaches to study the organic−inorganic hybrid nanocomposites, we carried out dansyl (5-dimethylaminonaphthalene-1-sulfonamide) fluorescence studies of the miscibility in MSSQ/P(MMA-*co*-DMAEMA) hybrid nanocomposites. This work is motivated in part by the recent studies that have shown that, in organic/inorganic hybrid nanocomposites, a large fraction of the polymer is influenced by the interfacial interactions.[20] Polymer behavior at the nanometer scale

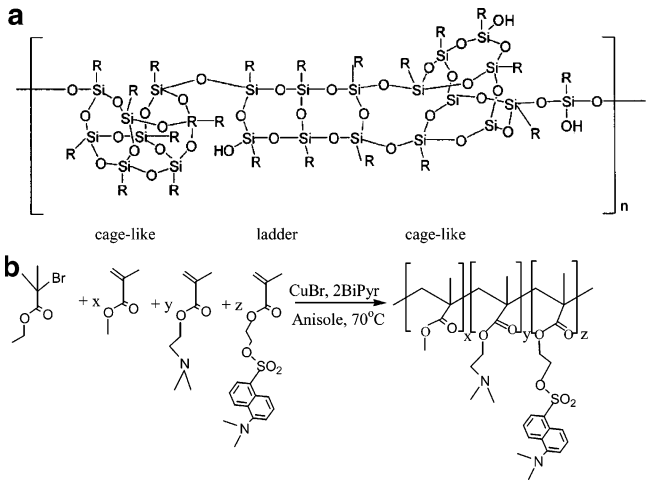

Figure 1. (a) Representative types of molecular structures in methyl silsesquioxane (MSSQ). (b) Synthesis of dansyl-labeled P(MMA-*co*-DMAEMA) by atom transfer radical polymerization (ATRP). BiPyr refers to 2,2′-bipyridine.

relevant to an interfacial region can be substantially different from that of the bulk polymers, as indicated by the higher T_g for polymer in the nanocomposites than in the bulk.[19a] A better understanding of the local environment found in these materials will give us the ability to prepare materials with controlled phase behavior or materials with controlled homogeneity for use in microelectronics and chemical sensors. Because the fluorescence emission energy of dansyl is strongly dependent on the polarity of its local environment, it can be used to study the interfacial structure of the organic/inorganic hybrid nanocomposites.[20] In this paper, we have chemically attached a small amount of fluorescent dansyl substituents into some of the methacrylate side chains. We report the effects of two variables, polymer loading and endgroup functionality of uncured MSSQ, on the fluorescence emission that affect the structure of the hybrid nanocomposites. We use the fluorescence signal from labeled polymers to monitor the local environment of polymers dispersed in MSSQ and the formation of polymer-rich domains due to phase separation.

Experimental Section

Materials. Two methyl silsesquioxane (MSSQ) prepolymer samples (see Figure 1a) from two different manufacturers were examined. MSSQ-HI (M_n = 1816; PDI = 3.46) and MSSQ-LO (M_n = 1625; PDI = 5.65) have similar molecular weights, as determined by gel permeation chromatography (GPC), and are distinguished primarily by the amount of silanol present in the uncured samples.[9] The designations MSSQ-HI and MSSQ-LO refer to resins with larger or smaller amounts of silanol groups, respectively. The former was obtained from Techniglas (GR-650) whereas the latter was produced by Dow Corning. Here PDI refers to the polydispersity index (M_w/M_n). The solvent propylene glycol methyl ether (PMOH, 98+%) was purchased from Aldrich Chemical Co. (Milwaukee, WI) and used as received.

Synthesis of Dansyl-Labeled P(MMA-*co*-DMAEMA). To synthesize the dansyl-labeled P(MMA-*co*-DMAEMA), we first prepared the functional monomer 1-dansyl methacrylate by reacting dansyl chloride with 2-hydroxyethyl methacrylate, which was catalyzed by triethylamine and 4-(dimethylamino pyridine) in dichloromethane at room temperature for 5 h. Subsequently,

(19) (a) Huang, Q. R.; Mecerreyes, D.; Hedrick, J. L.; Huang, E.; Kim, H.-C.; Volksen, W.; Frank, C. W.; Miller, R. D. *Macromolecules* **2003**, *36*, 7661. (b) Huang, Q. R.; Frank, C. W.; Mecerreyes, D.; Hedrick, J.; Volksen, W.; Miller, R. D. *Mater. Res. Soc. Symp. Proc.* **2002**, *726*, 211.

(20) (a) Ha, C.-S.; Park, H.-D.; Frank, C. W. *Chem. Mater.* **2000**, *12*, 839. (b) Goda, H.; Frank, C. W. *Chem. Mater.* **2001**, *13*, 2783. (c) Leezenberg, P. B.; Frank, C. W.; *Chem. Mater.* **1995**, *7*, 1784.

extraction, autoevaporation, and column chromatography were performed to purify the product (yield ~80%). Dansyl-labeled P(MMA-*co*-DMAEMA) was then prepared by controlled atom transfer radical polymerization (ATRP) (see Figure 1b). An initiator, ethyl 2-bromoisobutyrate; the catalyst, CuBr, 2,2′-bipyridine; and dansyl methacrylate were charged into a flask. The flask was then closed with a three-way stopcock and a vacuum-nitrogen cycle was repeated three times to remove the oxygen. Methyl methacrylate, dimethylaminoethyl methacrylate, and anisole were added using a syringe, and the reaction was heated at 70 °C for 3 h. To remove the copper catalyst, the polymer was diluted with THF and then passed through a small silica column, concentrated by solvent evaporation, and precipitated in hexanes. Finally, the copolymer was dried in a vacuum oven to constant weight. GPC analysis (polystyrene standard) shows $M_n = 3000$ g/mol, PDI = 1.20. The ^{1}H NMR result indicates that the dansyl-P(MMA-*co*-DMAEMA) copolymer contains 74 mol % MMA, 24 mol % DMAEMA, and 2 mol % dansyl-labeled MMA.

Film Preparation. Samples for fluorescence measurements were prepared as follows. Solutions of MSSQ and dansyl-P(MMA-*co*-DMAEMA) in PMOH (20 wt % solids) were loaded into a disposable syringe and filtered through a 0.2-μm Millex PTFE filter (Millipore, Inc) directly onto a clean single-polished ⟨100⟩ prime Si wafer. The coated substrate was spun at 3000 rpm for 30 s. Each sample was heated at 3 °C/min under argon to 180 °C and held for 2 h before cooling. The final film thicknesses ranged from 400 to 600 nm, depending on porogen loading.

Steady-State Fluorescence Measurements. The emission and excitation spectra of the hybrid nanocomposites were measured using a fluorescence spectrometer (FS 900CDT spectrometer, Edinburgh Instruments) with a 450-W steady-state xenon arc lamp. Films were excited in a front-face arrangement to minimize self-absorption. All spectra were taken with 0.5-mm slit widths and 0.5-s dwell time.

Time-Resolved Fluorescence Measurements. The system for fluorescence lifetime measurements has been described elsewhere.[21] The time-correlated single photon counting technique was used to measure fluorescence lifetime. In this approach, the frequency-doubled output of a Spectra Physics mode-locked, Nd:YAG laser was used to synchronously pump a dye laser, which was cavity dumped with a Bragg cell to produce a single pulse at 640 nm. The single pulse was then frequency doubled to give the excitation pulse, which typically had a duration of 10 ps at 320 nm, as detected by a Hamamatsu R1645U-01 microchannel plate detector. The instrument response at 320 nm was a Gaussian curve with a typical half-width of 50 ps.

Results

Dansyl, or 5-dimethylaminonaphthalene-1-sulfonamide, is a fluorescent dye that is mainly used as a solvatochromic probe because its emission is strongly influenced by its surrounding environment.[23] The energy of the emitting state of dansyl decreases (red-shifts) with the increase of solvent polarity. Because of this solvatochromic behavior, dansyl has been used to probe the microenvironment in volume phase transitions,[24] self-organizing systems,[25] surfaces,[26] and the biological systems.[27] Leezenberg and Frank showed that dansyl could also be used as a rigidochromic probe that monitored the local viscosity.[20c] They found that the rigidity strongly influenced dansyl fluorescence emission by hindering rearrangement of the naphthalene group and increasing the energy (blue shift), which is related to the twisted intramolecular charge-transfer character of 1-aminonaphthalenes in the excited state. The present study is focused on studying the phase separation behavior inside the MSSQ/P(MMA-*co*-DMAEMA) hybrid nanocomposites by taking advantage of the solvatochromic property of dansyl.

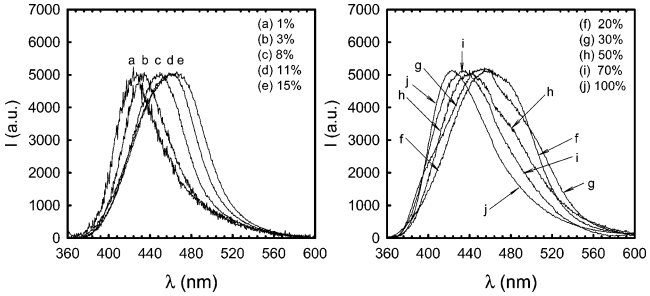

Figure 2. Fluorescence emission spectra of hybrid nanocomposites formed by dansyl-P(MMA-*co*-DMAEMA) with MSSQ-LO at different polymer loading levels cured at 180 °C.

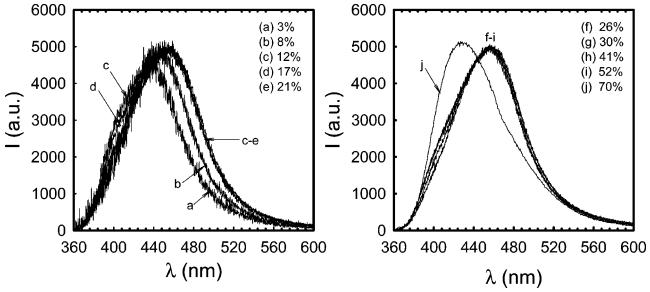

Figure 3. Fluorescence emission spectra of hybrid nanocomposites formed by dansyl-P(MMA-*co*-DMAEMA) with MSSQ-HI at different polymer loading levels cured at 180 °C.

Steady-State Fluorescence. Figures 2 and 3 show the fluorescence emission spectra for hybrid nanocomposites formed by dansyl-P(MMA-*co*-DMAEMA) with MSSQ-LO (Figure 2) and MSSQ-HI (Figure 3) cured at 180 °C as a function of dansyl-P(MMA-*co*-DMAEMA) loading. The excitation wavelength is 325 nm and all spectra are normalized to compare the fluorescence behavior within each system. Here, the dansyl fluorescent probe has been chemically attached to the PMMA side chain. Direct attachment is more attractive than simple dispersion because of the difficulty of controlling the precise location of a small probe within the matrix due to possible aggregation effects. For the MSSQ-LO/dansyl-P(MMA-*co*-DMAEMA) hybrid nano-

(21) (a) Leezenberg, P. B.; Marcus, A. H.; Frank, C. W.; Fayer, M. D. *J. Phys. Chem.* **1996**, *100*, 7646. (b) Stein, A. D.; Peterson, K. A.; Fayer, M. D. *J. Chem. Phys.* **1990**, *92*, 5622.
(22) Huang, E.; Toney, M.; Volksen, W.; Mecerreyes, D.; Brock, P.; Kim, H.-C.; Hawker, C. J.; Hedrick, J. L.; Lee, V. Y.; Magbitang, T.; Miller, R. D.; Lurio, L. B. *Appl. Phys. Lett.* **2002**, *81*, 2232.
(23) (a) Reichardt, C. *Chem. Rev.* **1994**, *94*, 2319. (b) Leezenberg, P. B. Ph. D Thesis, Stanford University, 1994.
(24) (a) Hu, Y.; Horie, K.; Ushiki, H. *Macromolecules* **1992**, *25*, 6040. (b) Hu, Y.; Horie, K.; Ushiki, H. Tsunomori, F.; Yamashita, T. *Macromolecules* **1992**, *25*, 7324.
(25) Seo, T.; Take, S.; Miwa, K.; Hamada, K.; Ijima, T. *Macromolecules* **1991**, *24*, 4255.
(26) (a) Holmes-Farley, S. R.; Whiteside, G. *Langmuir***1986**, *2*, 266. (b) Lochmuller, C. H.; Marshall, D. B.; Wilder, D. R. *Anal. Chim. Acta* **1981**, *130*, 31. (c) Lochmuller, C. H.; Marshall, D. B.; Harris, J. M. *Anal. Chim. Acta* **1981**, *131*, 263.
(27) Ghiggino, K. P.; Lee, A. G.; Meech, S. R.; O'Connor, D. V.; Phillips, D.; *Biochemistry* **1981**, *20*, 5381.

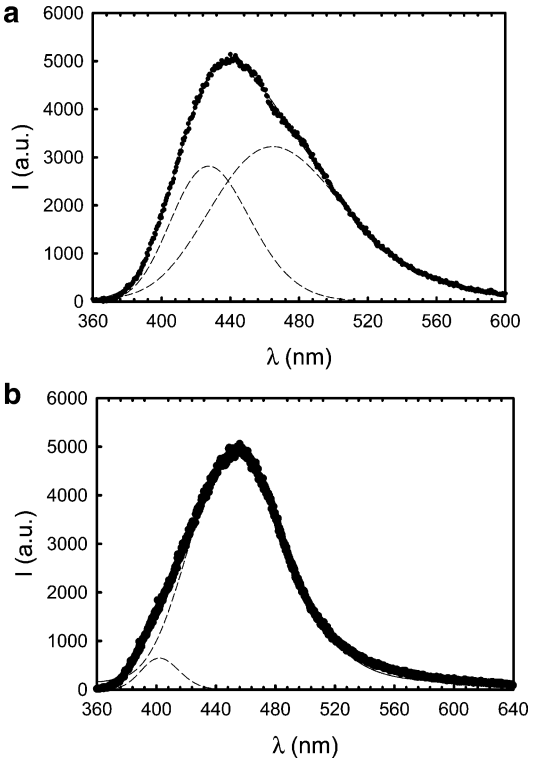

Figure 4. Deconvolution of fluorescence emission spectra for hybrid nanocomposites formed by dansyl-P(MMA-*co*-DMAEMA) with MSSQ-LO (a) and MSSQ-HI (b) cured at 180 °C. Both hybrids contain 50 wt % dansyl-P(MMA-*co*-DMAEMA). The solid circles are experimental data, the solid curves are overall fits, and the dashed curves are two-Gaussian fits.

composites shown in Figure 2, at low polymer loading (<20 wt %), the emission spectra shift to lower frequency (red-shift) with increasing polymer loading, and the bandwidth increases, which may be attributed to a larger distribution of environments experienced by the dansyl chromophore. Further increases in polymer loading to above 20 wt % cause the appearance of a second band centered at higher frequency. The peak position of the emission spectrum of pure dansyl-P(MMA-*co*-DMAEMA) is located at ~417 nm. For the MSSQ-HI/dansyl-P(MMA-*co*-DMAEMA) hybrid nanocomposites shown in Figure 3, at polymer loading levels lower than 21 wt %, similar to MSSQ-LO, the emission spectra also red-shifts. However, the emission spectra are nearly unchanged for polymer loading level ranging from 21 to 52 wt % before blue-shifting to ~417 nm at 70 wt % loading level. The emission spectrum of the hybrid with 70 wt % polymer loading is very similar to that of the pure dansyl-P(MMA-*co*-DMAEMA) (see curve j in Figure 2).

To have a clear comparison between MSSQ-HI and MSSQ-LO, we fit the emission spectra of the hybrid nanocomposites formed by dansyl-P(MMA-*co*-DMAEMA) with MSSQ-LO (Figure 4a) and MSSQ-HI (Figure 4b) with two Gaussian bands, as shown in Figure 4. Both nanocomposites contain 50 wt % dansyl-P(MMA-*co*-DMAEMA). The two Gaussian bands correspond to the relative populations of dansyl in two different local environments. The low-energy band, which dominates at low polymer loading, is reasonably attributed to the local environment of dansyl surrounded by the MSSQ phase; in contrast, the high-energy band, which becomes significant at high polymer loading,

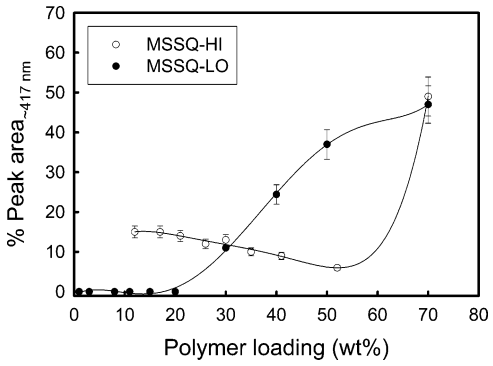

Figure 5. Percent area of high-energy bands as a function of polymer loading for hybrid nanocomposites formed by dansyl-P(MMA-*co*-DMAEMA) and MSSQ-LO (●) and MSSQ-HI (○) cured at 180 °C.

may originate from the local environment of dansyl surrounded by the P(MMA-*co*-DMAEMA) phase. Figure 4 clearly indicates that the contribution from the high-energy band for MSSQ-LO is significantly larger than that for MSSQ-HI, suggesting the formation of larger polymer domains inside the MSSQ-LO matrix, which ultimately transform into larger pores upon polymer burnout. This conclusion is consistent with our previous SAXS,[9b] TEM,[19a] and pyrene excimer fluorescence results.[19]

By deconvolution of the fluorescence emission spectra, we can obtain the relative peak areas and peak frequencies. Figure 5 shows the plot of the percentage of the area for the fluorescence emission band centered at high-energy (e.g., ~417 nm) as a function of polymer loading for both MSSQ-LO (solid circles) and MSSQ-HI (empty circles). For MSSQ-LO hybrid nanocomposites, at low loading levels (<20 wt %), the emission spectra are fitted reasonably well by one Gaussian, which suggests the dansyl probes are mainly surrounded by the MSSQ phase. With the increase of polymer loading to above 20 wt %, two Gaussians are needed to obtain good fits, and the percentage of areas of the high-energy band increases with polymer loading, which may indicate the formation of larger polymer domains. By contrast, MSSQ-HI hybrid nanocomposites behave very differently with small shoulders located at ~400 nm appearing in the emission spectra even at polymer loading levels as low as 12 wt %. The %Peak areas decrease slightly with polymer loading at loading level <52 wt % before increasing dramatically.

The behavior of the high-energy band for MSSQ-HI hybrids at loading level <50 wt % is not completely understood. It is hard to imagine that the polymer domain sizes at 10 wt % polymer loading can be larger than those at 50 wt % loading. Since the contribution from this high-energy band at this loading range is relatively small (between 9 and 15%) and the peak frequency is located at higher value (~401 nm) than that of pure dansyl-P(MMA-*co*-DMAEMA), this high-energy emission band may be due to the heterogeneity of the functional group inside MSSQ-HI, which causes the formation of a small amount of either unusually rigid or hydrophobic shell surrounding the dansyl probes. Note that the dansyl emission behavior can also be strongly influenced by the local rigidity.[20c] If a dansyl probe is locked in a rigid environment, solvent dipoles may not relax around the excited molecules and lower its emission. In addition, a

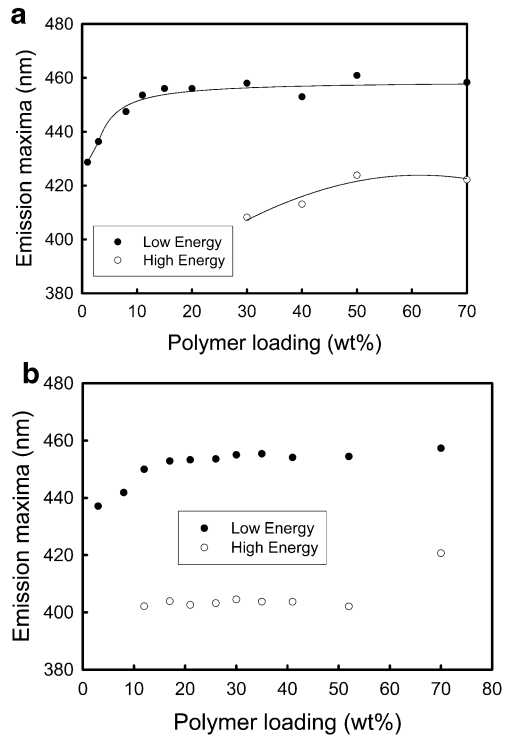

Figure 6. Emission maxima as a function of polymer loading for hybrid nanocomposites formed by dansyl-P(MMA-*co*-DMAEMA) and MSSQ-LO (a) and MSSQ-HI (b) cured at 180 °C.

rigid environment may also hinder the arrangement of the dimethylamino and naphthalene groups, preventing relaxation and causing emission from a higher energy state.[20c] The significant increase in %Peak area at 70 wt % loading may indicate the formation of larger polymer domains because, at this loading level, dansyl-P(MMA-*co*-DMAEMA) changes from the minority phase to the majority phase, thus exhibiting phase reversal.

Figure 6 shows the emission maxima of the emission peaks for both high- and low-energy bands for hybrid nanocomposites formed by dansyl-P(MMA-*co*-DMAEMA) with MSSQ-LO (Figure 6a) and MSSQ-HI (Figure 6b) cured at 180 °C. Both MSSQ-HI and MSSQ-LO show significant red-shifts for the low energy band as polymer concentration increases from 0 to 12 wt % before reaching a steady state at ~455 nm. As noted above, this low-energy band corresponds to the local environment of dansyl surrounded by the MSSQ phase. Since MSSQ is intrinsically hydrophobic, with its hydrophobicity originating from the methyl group in MSSQ, the red-shift in the low-energy band, which is related to the local polarity increase, may indicate the dansyl-P(MMA-*co*-DMAEMA) distributes preferentially into the −O−Si−O− region over the $-CH_3$ region. Whereas the high-energy band also shows a red-shift, the main difference between MSSQ-LO and MSSQ-HI is that, for MSSQ-LO, the red-shift starts at ~30 wt % loading before reaching steady state at 50 wt %. For MSSQ-HI, in contrast, the peak position remains constant and the red-shift only occurs for loading levels above 50 wt %. For both MSSQ-HI and MSSQ-LO, the peak frequency at 70 wt % loading level is ~418 nm, corresponding to that of pure dansyl-P(MMA-*co*-DMAEMA), which again suggests the formation of large polymer domains.

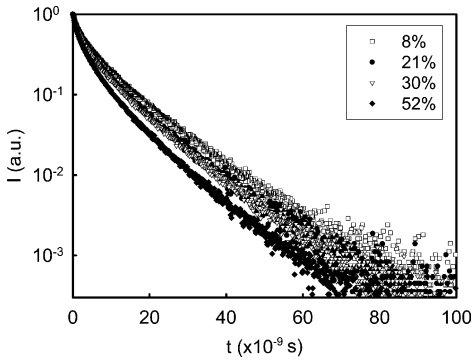

Figure 7. Fluorescence decay profiles for MSSQ-HI/dansyl-P(MMA-*co*-DMAEMA) hybrid nanocomposites cured at 180 °C with different polymer loading levels: (□) 8 wt %; (●) 21 wt %; (▽) 30 wt %; and (◆) 52 wt %.

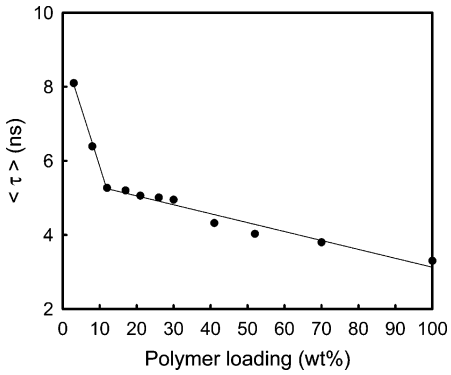

Figure 8. Plot of average lifetime $<\tau>$ versus polymer loading for MSSQ-HI/P(MMA-*co*-DMAEMA) hybrid nanocomposites cured at 180 °C.

Time-Resolved Fluorescence. Figure 7 shows the time-resolved fluorescence decay curves for MSSQ-HI/dansyl-P(MMA-*co*-DMAEMA) hybrid nanocomposites cured at 180 °C. The time-resolved fluorescence intensity can be satisfactorily fitted with single William−Watts (WW) stretched exponential function given by

$$I(t) = I_0 \exp[-(t/\tau)^{\beta}] \quad (1)$$

Here I_0 represents the preexponential factor, τ is the excited-state lifetime, and β is the distribution parameter originating from the distribution of local environments of dansyl probes surrounded by MSSQ phase. For a uniform local environment of dansyl, $\beta = 1.0$. For a distribution of dansyl local environments, $0 < \beta < 1$. The average excited-state lifetimes $<\tau>$ are calculated by using

$$<\tau> = \tau\frac{\Gamma(1/\beta)}{\beta} \quad (2)$$

where $\Gamma(x)$ is a Γ function.

Figure 8 summarizes the effects of polymer loading on the dansyl time-resolved fluorescence intensity decay kinetics within the MSSQ-HI/dansyl-P(MMA-*co*-DMAEMA) hybrid nanocomposites cured at 180 °C. Before 12 wt % polymer loading level, the average excited-state lifetime $<\tau>$ decreases significantly with polymer loading level. The decrease in $<\tau>$ then becomes more gradual with further increases in polymer loading, and $<\tau>$ eventually reaches 3.3 ns for pure dansyl-P(MMA-*co*-DMAEMA). Since the fluorescence transient decays were monitored at 460 nm, which reflects the local environments of dansyl probes

surrounded by the MSSQ phase, the decrease in $<\tau>$ suggests the increase in polarity of local environments of dansyl surrounded by MSSQ phase and is consistent with the steady-state fluorescence results discussed previously.

Discussion

The phase separation behavior of organic/inorganic hybrid nanocomposites is determined by the thermodynamics of phase separation in a two-component system as well as by kinetic factors, and the formation of nanoscale polymer domains inside the organosilicate matrix can only be achieved by using components (porogen + resin) that initially strongly interact with each other by hydrogen bonding or other attractive forces.[28] Our previous FTIR results showed that strong hydrogen bonding interactions occur between the −SiOH end groups in MSSQ and the tertiary amino substituents in P(MMA-*co*-DMAEMA) in films at 25 °C.[9] Thus, MSSQ and P(MMA-*co*-DMAEMA) readily form nanocomposites.

The structure and morphology of nanocomposites formed by methyl silsesquioxane (MSSQ) and poly(methyl methacrylate-*co*-dimethylaminoethyl methacrylate) [P(MMA-*co*-DMAEMA)] have recently been studied by several techniques, such as small-angle X-ray scattering (SAXS),[9b,22] atomic force microscopy (AFM),[9] modulated differential scanning calorimetry (MDSC),[19a] pyrene excimer fluorescence spectroscopy,[19] transmission electron microscopy (TEM),[13a,19a] small-angle neutron scattering,[13a] and field-emission scanning electron microscopy (FE-SEM).[22] It has been found that copolymers containing 20 to 30 mol % of DMAEMA comonomer provide optimal coatings and foaming efficiencies.[9] An important materials design element is that there exist strong hydrogen bonding interactions between the −OH end groups in MSSQ and the tertiary amino groups in P(MMA-*co*-DMAEMA) in films before the silanol cross-links. In addition, the amino substituent in P(MMA-*co*-DMAEMA) can act as a catalyst for the condensation and cross-linking of MSSQ. MDSC results show only a single observable glass transition temperature (T_g) in all the hybrid nanocomposites with P(MMA-*co*-DMAEMA) loading level up to 70 wt %, which is an indication of the apparent miscibility at the length scale of 10 nm and above.[19a] In contrast, pyrene excimer fluorescence, which occurs when an electronically excited-state pyrene approaches within ∼4 Å of a ground-state pyrene in a proper geometry, provides an alternate probe of the hybrid nanocomposites formed with MSSQ and pyrene-labeled P(MMA-*co*-DMAEMA). The pyrene fluorescence results reveal that pyrene excimer formation occurs at P(MMA-*co*-DMAEMA) loading levels above 6 wt %, and the excimer-to-monomer (I_E/I_M) ratio increases with polymer loading. At a fixed polymer loading, the higher the initial silanol concentration in the uncured MSSQ, the larger the I_E/I_M ratio, suggesting the greater immiscibility. The pyrene excimer fluorescence is limited by the fact that it is insensitive to hybrid nanocomposites with polymer domain sizes larger than ∼5 nm as determined by SANS.[19a] The pyrene excimer fluorescence results also suggest that both increasing polymer loading and decreasing silanol concentration of the uncured MSSQ cause greater immiscibility between MSSQ and P(MMA-*co*-DMAEMA), which ultimately translates into larger pores upon porogen burnout, as evidenced by the TEM,[13a,19a] FE-SEM, and SAXS.[22] However, none of the above approaches provides the information about the location of the polymer inside the MSSQ matrix.

The change in the micropolarity surrounding the dansyl probes can induce changes in the emitting states of the dansyl groups. Thus, the solvatochromic properties of dansyl groups provide us a new route to study the phase separation behavior in the organic/inorganic hybrid nanocomposites. Dual peak emission behavior similar to that of these MSSQ hybrids was also observed for the poly(dimethylsiloxane) (PDMS)/silica nanocomposites.[20c] In that paper, the two emission bands were interpreted as due to the existence of dansyl probes in two different local environments: the low-energy emission band at around ∼460 nm was related to the local environment of dansyl probes unaffected by the silica phase; on the other hand, the high-energy band located at ∼390 nm was caused by the dansyl groups that were surrounded by the more rigid and polar interface. A similar interpretation is also applicable to MSSQ/P(MMA-*co*-DMAEMA) hybrid nanocomposites. The dansyl probes may exist in two different local environments: the hydrophobic P(MMA-*co*-DMAEMA) domains and the rigid but "polar" MSSQ (because dansyl may locate preferentially close to −O−Si−O− rather than methyl group) phase. For a particular polymer loading range, there exists an interfacial region at the polymer-MSSQ boundary in which polymer molecules interpenetrate the MSSQ matrix, or the mixed purity domains, rather than two pure individual components. The phase purity in a phase-separated nanocomposite can be discovered by monitoring the dansyl emission band shift, as shown in Figure 6. For MSSQ-LO hybrids with 30 wt % polymer loading, the high-energy band peak frequency is located at a higher value than that with 70 wt % polymer loading, suggesting that the local environments of the dansyl for the former are less mobile than that of the latter. In addition, the increase of %Peak area for the high-energy band in MSSQ-LO hybrid nanocomposites as shown in Figure 5, which may suggest the increase in polymer domain size, is also consistent with the SANS results on similar systems but with partially deuterated P(MMA-*co*-DMAEMA).[13a] The larger polymer domain size at higher polymer loading is easy to understand because, as P(MMA-*co*-DMAEMA) loading increases, less chain extension of MSSQ will occur before phase separation is thermodynamically favored. This trend continues until the P(MMA-*co*-DMAEMA) loading is high enough to cause phase inversion, with MSSQ dispersing in a P(MMA-*co*-DMAEMA) matrix. At lower degree of chain extension, the viscosity of the system is also lower, which allows greater migration of P(MMA-*co*-DMAEMA) through the matrix to form larger phase-separated domains.

Summary and Conclusions

In summary, we have carried out both steady-state and time-resolved fluorescence studies on the phase separation

(28) Chujo, Y.; Saegusa, T. *Adv. Polym. Sci*. **1992**, *100*, 11.

behavior of cross-linked MSSQ/P(MMA-*co*-DMAEMA) hybrid nanocomposites, in which the polymer domain structures are similar to the final pore morphology upon polymer burnout. We have covalently attached dansyl probe molecules to the non-nitrogeneous methacrylate side chain in P(MMA-*co*-DMAEMA) copolymer at a ∼2 mol % level, and used the solvatochromic properties of dansyl to examine the morphology of dansyl-P(MMA-*co*-DMAEMA)/MSSQ nanocomposites. Two different resins, MSSQ-HI and MSSQ-LO, were used to study the effect of silanol concentration in the uncured MSSQ on the phase separation behavior of the hybrid nanocomposites. Two emission bands were observed on the dansyl fluorescence spectra: the high-energy band was interpreted as due to the hydrophobic P(MMA-*co*-DMAEMA) domain, and the low-energy band was due to the rigid but relatively "polar" MSSQ (−O−Si−O−) phase. Dansyl fluorescence results show the significant difference between MSSQ-HI and MSSQ-LO. In MSSQ-HI nanocomposites, a phase-mixed domain dominates the emission spectra up to 50 wt %, and a significantly larger value for the high-energy peak frequency suggests that the dansyl is tightly locked in the rigid MSSQ-HI matrix. In contrast, MSSQ-LO nanocomposites phase separate at ∼30 wt % and pure dansyl-P(MMA-*co*-DMAEMA) phase forms at ∼50 wt % polymer loading level. For the low-energy band, decreases in both emission energy and average excited-state lifetime suggest that the dansyl molecules distribute preferentially around the polar −O−Si−O− rather than around methyl groups in MSSQ. The %Peak area for the high-energy band increases with polymer loading, implying the formation of larger polymer domains. This study suggests that both increasing the polymer loading level and lowering the amount of silanol endgroup in the uncured MSSQ promote phase separation in the hybrid nanocomposites. This is because the probe molecules avoid the boundary region and seek a polymer-rich environment, resulting in the formation of larger polymer domains that ultimately transform into larger size pores upon polymer burnout. The conclusion has been verified by previous SANS, SAXS, and TEM results.

Acknowledgment. We thank Mr. Hu Cang for the technical assistance in lifetime measurements and Dow Corning Corporation for the preparation of the MSSQ-LO samples. This work was supported by the NIST Advanced Technology Program (contract 70NANB8H4013).

CM048774S